technologies

MDPI

Article

Image-Label Recovery on Fashion Data Using Image Similarity from Triple Siamese Network

Debapriya Banerjee *, Maria Kyrarini and Won Hwa Kim

Department of Computer Science and Engineering, The University of Texas at Arlington (UTA), Arlington, TX 76019, USA; maria.kyrarini@uta.edu (M.K.); won.kim@uta.edu (W.H.K.)
* Correspondence: debapriya.banerjee2@mavs.uta.edu

Abstract: Weakly labeled data are inevitable in various research areas in artificial intelligence (AI) where one has a modicum of knowledge about the complete dataset. One of the reasons for weakly labeled data in AI is insufficient accurately labeled data. Strict privacy control or accidental loss may also cause missing-data problems. However, supervised machine learning (ML) requires accurately labeled data in order to successfully solve a problem. Data labeling is difficult and time-consuming as it requires manual work, perfect results, and sometimes human experts to be involved (e.g., medical labeled data). In contrast, unlabeled data are inexpensive and easily available. Due to there not being enough labeled training data, researchers sometimes only obtain one or few data points per category or label. Training a supervised ML model from the small set of labeled data is a challenging task. The objective of this research is to recover missing labels from the dataset using state-of-the-art ML techniques using a semisupervised ML approach. In this work, a novel convolutional neural network-based framework is trained with a few instances of a class to perform metric learning. The dataset is then converted into a graph signal, which is recovered using a recover algorithm (RA) in graph Fourier transform. The proposed approach was evaluated on a Fashion dataset for accuracy and precision and performed significantly better than graph neural networks and other state-of-the-art methods.

Keywords: semisupervised learning; metric learning; signal recovery

check for updates

Citation: Banerjee, D.; Kyrarini M.; Kim, W.H. Image-Label Recovery on Fashion Data Using Image Similarity from Triple Siamese Network. *Technologies* **2021**, *9*, 10. https://doi.org/10.3390/technologies9010010

Academic Editors: Abdellah Chehri and Pedro Antonio Gutiérrez
Received: 31 October 2020
Accepted: 15 January 2021
Published: 21 January 2021

1. Introduction

Supervised learning [1,2] is an approach in Machine Learning (ML) for classification [3] or regression tasks [4], where a set of labeled data is used to train a prediction model. However, in practice, obtaining sufficient labeled data for training a model can be difficult. There may be a strict privacy-control policy that restricts one from obtaining labeled data or human error that can cause false or missing labels in the dataset. Additionally, there may not be enough of a budget to obtain all information labeled by human annotators, especially when expert knowledge is needed for the annotations. For example, during the COVID-19 pandemic, online shopping drastically increased, and shop owners needed to update their products. Manually finding the category of each product is time-consuming, therefore, it is important to develop a framework that can automatically categorize new data on the basis of a small amount of labeled data. In this scenario, an approach called Semisupervised Learning (SSL) can be useful to solve the problem of weakly labeled data. SSL algorithms are applied in such cases where a very limited amount of label data along with a large number of unlabeled data are used as input. SSL algorithms learn a better prediction rule than supervised ML would learn if trained only on a small amount of label data. Considering this approach in mind, we designed a semisupervised framework to detect the labels or categories of unlabeled data. The concept behind our approach is that similar data points lie very close to each other in vector space. In this regard, our objective was to learn a similarity measure to detect the distance of data points in vector space and then detect the labels of unlabeled data through label propagation.

Distance metric learning (DML) is a popular concept in modern ML research to learn a similarity measure between two entities. DML aims at automatically constructing task-specific distance metrics from data in an ML manner. It is often difficult to design metrics that are well-suited to the particular data and task of interest. In this work, we designed a novel DML model to detect the distance between every two images in an image dataset with fashion products called the Fashion dataset [5], and then we propagated the label information from a small subset of labeled data to the entire set of unlabeled data. It was assumed that similar objects have a distance very close to zero and they share the same label information. Figure 1 shows a visual representation of when similar objects share the same label information.

The second component, label propagation, is a popular problem in SSL, where a small subset of data points has label information, and the challenge is to propagate labels to the unlabeled points from the labeled points through an algorithm. We adopted a method introduced in [6] that exploits graph harmonics and sparse coding of graph signals in the dual space of the graph. Here, we consider the labels of images as the graph signal on their nodes, and the metric learned by DML consists of the edge between nodes (i.e., images). In the end, our pipeline predicts the image labels of the entire dataset on the basis of a small subset of images with given labels.

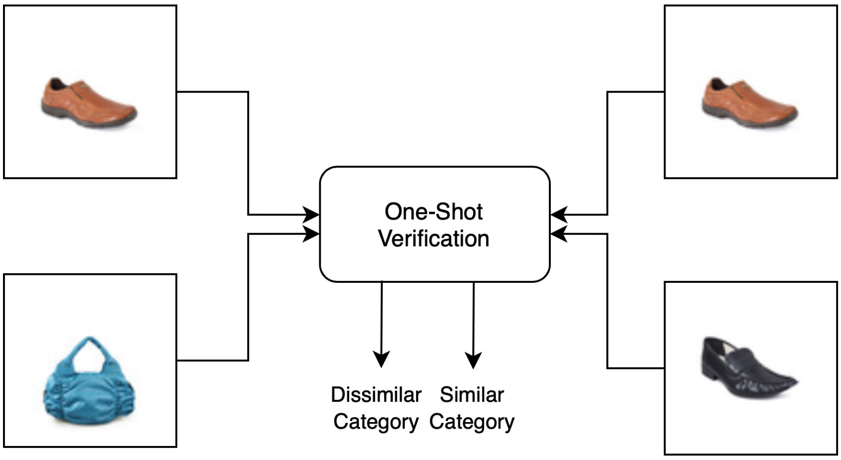

Figure 1. Visual representation of basic intuition.

In this work, we designed a novel approach combining DML and label propagation for SSL. Our contributions are summarized as follows:

- Designing a novel DML model to learn good similarity measures between every two images in an image dataset and create a graph with their distances.
- Recovering labels for all images from the graph using a label-propagation algorithm.

The rest of the paper is structured as follows: Section 2 describes related work, Section 3 describes preliminary works that we performed as part of our experiments, Sections 4 and 5 present our proposed methodology and implementation, and Section 6 discusses the numerical experiments.

2. Related Work

SSL [7] is an algorithm family that falls between supervised [1,2] and unsupervised learning, making use of labeled and unlabeled data to perform learning tasks. For SSL, a smaller set of labeled data in combination with a large set of unlabeled data are typically used for the construction of a better learning technique. In recent years, due to the lack of labeled data, SSL gained more popularity than supervised learning. Our model gained inspiration from recent works on distance metric learning and label-propagation algorithms. We provide a brief overview of the related work in both of these areas.

Label propagation is a way in which SSL detects the labels of unlabeled observations. Inductive learning [8] regards learning general rules for making predictions, while transductive learning learns prediction rules from training data for specific testing data. SSL is transductive, as labels are gradually predicted, and the model has to be retrained whenever the testing set changes. In our case, labels were propagating, and if a new instance (i.e., graph node) was added, the model had to be run again, so it was transductive. Puy et al. [9] first proposed the random sampling of band-limited signals on graphs. Later, Kim et al. [10] proposed adaptive signal recovery on graphs via harmonic analysis for experimental design in neuroimaging. Bronstein et al. [11] prepared an exhaustive literature review paper, "geometric deep learning: going beyond Euclidean data", on this topic. Malkov et al. [12] first introduced the nearest-neighbor search using small world problem. Saito et al. [13] proposed a semisupervised domain adaption technique via minimax entropy. Later, Zhai et al. [14] proposed a self-supervised SSL where they bridged the gap between self-supervised and SSL.

Work on one-shot and few-shot learning has gained popularity in DML. One-shot learning is a learning task where there might be only one training example for a label or category, and few-shot learning can be applied where there are only a few training examples available for each label. One-shot learning is a way of learning similarity measures, and it was first introduced by Bromley et al. [15] for signature verification using a Siamese time-delay neural network. Then, Fei-Fei et al. [16] proposed a one-shot-based approach for object categories. The authors assumed that currently learned classes can help to make predictions on new ones when just one or few labels are available. Lake et al. [17] presented a hierarchical Bayesian model that reached human-level error on few-shot learning alphabet-recognition tasks. Koch et al. [18] presented a deep-learning model based on computing the pairwise distance between samples using Siamese networks, and Vinyals et al. [19] presented end-to-end trainable k-nearest neighbors using cosine distance. Schroff et al. [20] proposed an anchor-based triple network for unified embedding called FaceNet, which is useful for face recognition and clustering. The FaceNet model is trained on the triplet loss function. Kertész et al. [21] proposed multidirectional image-projection transformation with fixed vector lengths (MDIPFL) for one-shot learning, which performed significantly better.

Many recent works on SSL were based on generative models with deep neural networks. Few of such examples are graph neural networks (GNN) [22], variational autoencoders [23,24], and generative adversarial networks [25–27]. A GNN is a deep-learning approach to deal with graph-structured data, and it was first proposed by Gori et al. [22]. Kim et al. [6] proposed a select-recovery-based model to recover multivariate signals in an online manner using graph-signal processing. Kipf and Welling [28] proposed deep-learning-based GNN models on semisupervised classification problems. Chang et al. [29] develop graph interaction networks that learn pairwise particle interactions and apply them to discrete particle-physical dynamics. Duvenaud et al. [30] and Kearnes et al. [31] studied molecular fingerprints using variants of the GNN architecture, and Gilmer et al. [32] further developed the model by combining it with set representations. Vinyals et al. [19] showed state-of-the-art results on molecular prediction. Appalaraju et al. [33] proposed a Siamese-network-based deep CNN model using curriculum learning and transfer learning for image-similarity measurements.

Our method is based on the combination of DML and a label-propagation algorithm. We used a one-shot-learning [18,19] approach to learn DML and construct graphs on the basis of distance learned from DML. Unlike traditional one-shot learning networks, we propose a novel DML network that we combined with a label-propagation algorithm to achieve the best results.

3. Preliminary Work

We focused on the Fashion dataset [5], which was downloaded from an online fashion e-commerce store called Myntra. Although we focused on this dataset, this approach can be applied to other image datasets or modalities. The fashion data consisted of a set of images of fashion products with their label information. Each of these images was processed to grayscale and resized to 105 × 105 pixels. It was then processed to extract features.

The one-shot-learning approach is a very popular technique to learn domain-specific features from input images when the number of input images per class is limited. This technique is very useful, even for DML, when the similarity measure is to be calculated between input images. In this work, we used this approach as our baseline model to calculate a good similarity measure between images. Koch et al. [18] focused on a twin Siamese network to perform DML, and then reused that network's features for one-shot learning without any retraining.

A twin Siamese network performs well for one-shot learning tasks, but training this network is a time-consuming process. While training this network, it takes two inputs at a time and calculates a similarity score from their distances. Therefore, the number of comparisons was more ($(\binom{N}{k})$ for N number of images and k is 2) to calculate the distance of all images in our dataset. This twin Siamese network is sensitive with respect to context and fails to capture fine-grain differences between two images. The above-mentioned problems motivated us to focus on DML, creating a novel network that quickly converges and captures fine-grained differences of labels.

4. Proposed Methodology

In this section, we discuss the design approach we propose. SSL is an approach where a learning algorithm requires a small amount of training data and a large amount of unlabeled data. Our goal in this research is to learn a prediction rule to detect the labels of unlabeled datasets with the help of a small amount of labeled data points. We divided our algorithm into two steps: distance metric learning and label propagation.

4.1. Distance Metric Learning

DML focuses on automatically constructing domain-specific distance metrics from supervised data. In this step, our framework learns a good similarity measure between two images. There are a few popular standard distance metrics, e.g., Euclidean distance and cosine similarity, where we need prior knowledge of the domain. The aim of DML is to construct a task-specific distance metric from a particular dataset.

Twin Siamese networks are one of the ways of learning distance between two images. The concept of a twin Siamese network is that there are two parallel networks that share the same weights. These two parallel networks are basically identical and learn the encoding of input images. We used the twin Siamese network as our baseline model.

Our baseline model is a convolutional neural network (CNN) version of the twin Siamese network, which takes two input images and learns the encoding of two input images through this twin network. In the end, it learns the L_1 distance of two feature vectors and produces a distance score between 0 and 1 through a sigmoid layer. The detailed architecture of this network is as follows: the model consists of a sequence of convolutional layers, each of which uses a single channel with filters of varying size. The network applies a rectified linear unit (ReLU) activation function to the output feature maps, followed by max-pooling with a filter size and stride of 2.

Twin Siamese networks perform well compared to all other DML mentioned in Section 2. However, Twin Siamese network performance is very slow. The convergence time of this network is extremely large, taking almost 2000 epochs to converge. Detailed hardware specifications are provided in Section 5.3. If we have an N number of images in the dataset, the number of comparisons that happen in this network is $\binom{N}{k}$, which is very large to obtain the distance of every pair of images in our dataset. Therefore, we propose the concept of a triple Siamese network to optimize these points.

4.1.1. Triple Siamese Network

In this network, we used three parallel networks that shared the same weights. The architecture of each network is the same CNN network as the one that we used in the twin

Siamese network. Through this network, we learned the similarity function as $f(x_1, x_2)$, where $f(x_1, x_2) = ||h(x_1) - h(x_2)||_2$, here x_1 and x_2 are input images to the network, and $h(x_1)$ and $h(x_2)$ are the encoding of x_1 and x_2 by the CNN. Figure 2 shows the system architecture of the triple Siamese network.

This network takes three images (x_1, x_2, x_3) as input in such a way that x_2 and x_1 are taken from the same class, and x_2 and x_3 are taken from different classes. The goal is to maximize the distance between x_2 and x_3, and minimize the distance between x_2 and x_1. This network learns two L_2 distances from these two pairs at a time.

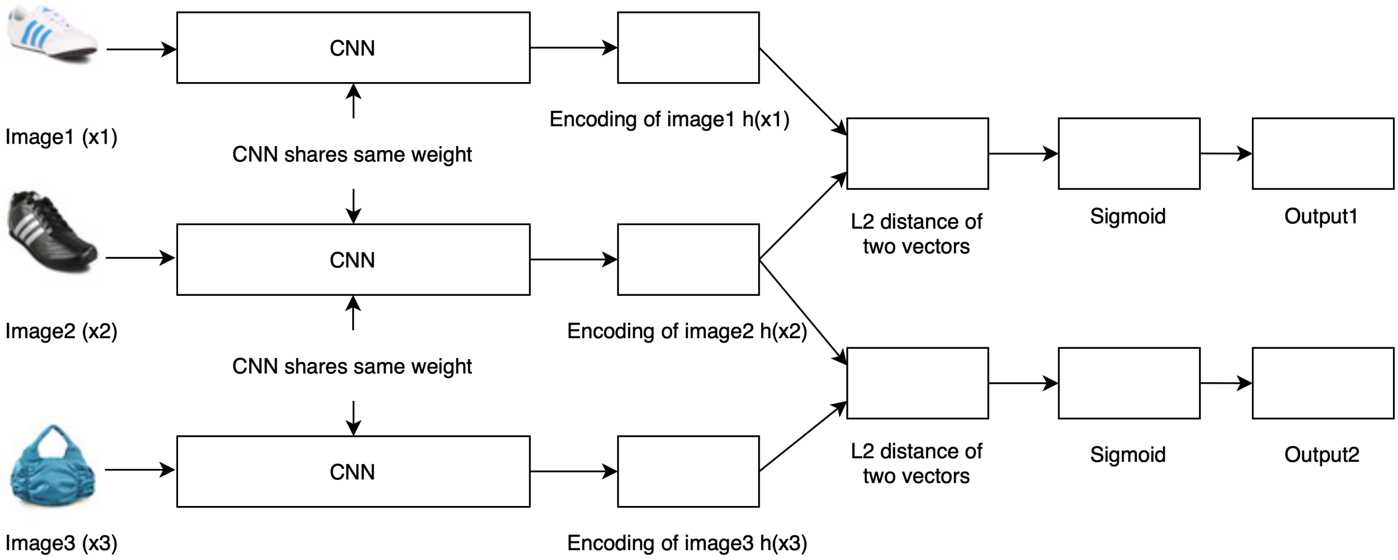

Figure 2. Triple Siamese network.

4.1.2. Graph Representation

After the triple Siamese Network provided the distance of each pair of images in the Fashion dataset, we graphically represented our data. We have graph $G = \{V, E\}$, where V is a set of images, and E is the set of distances of each pair of images. Hence, $V = \{v_1, v_2 \ldots v_N\}$, $E = \{e_{ij}$, where $e_{ij} = \text{dist}(v_i, v_j)\}$, and N = total number of images. Figure 3 displays a graphical representation of the Fashion dataset [5].

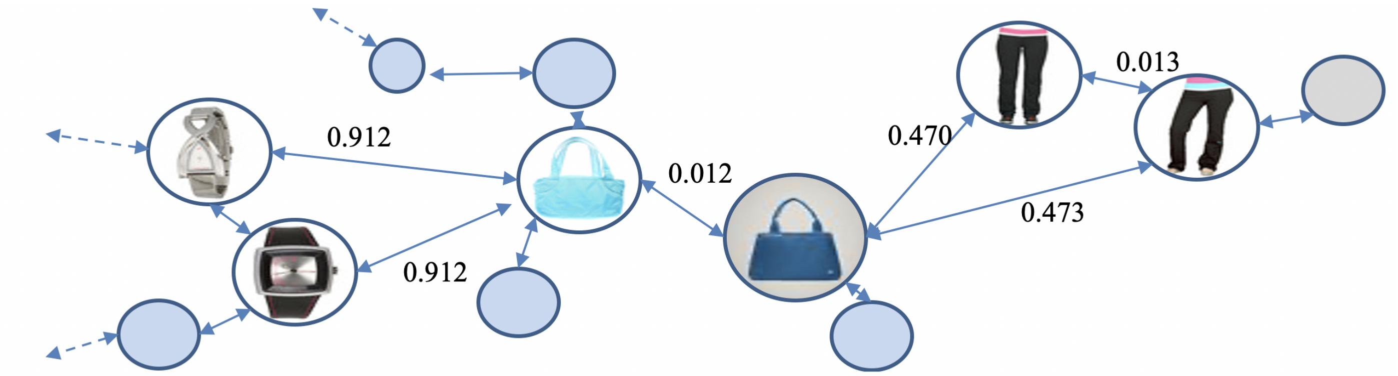

Figure 3. Graphical representation of image dataset.

4.2. Label Propagation

Label propagation determines the labels of unlabeled data from a very small amount of labeled data. In this project, we considered the graph as graph signal and ran the RA (Kim et al. [6]) on the graph. We recovered the graph signal using the harmonic analysis of the graph. We applied two useful concepts, spectral graph theory [34] and harmonic analysis of the graph [6,10], for our RA.

4.2.1. Spectral Graph Theory

Spectral graph theory [34] is the study of the properties of a graph in relationship to the eigenvalues and eigenvectors of matrices associated with the graph, such as its distance matrix or Laplacian matrix. Graph $G = \{V, E\}$ is represented by a set of vertices V of size N and a set of edges E that connect the vertices. Another matrix, graph Laplacian $L = D - W$, where a degree matrix $D_{N \times N}$, is a diagonal matrix with the ith diagonal element being the sum of edge weights connected to the ith vertex and $W_{N \times N}$ being a distance matrix where it is the most common way to represent a graph G, where each element d_{ij} denotes the distance between the ith and jth vertices.

4.2.2. Graph Harmonic Analysis

Graph harmonic analysis [6,10] utilizes the Fourier/wavelet transform of the original signal and filters in the frequency domain. The reason behind using harmonic analysis is making use of sparsity in terms of representation obtained in the Fourier/wavelet space of the graphs. By constructing different shapes of band-pass filters in the frequency space and transforming them back into the original space, we can construct a mother wavelet ψ on the nodes of a graph coming from its representation in the frequency space. For this implementation, using spectral graph theory, we used orthonormal bases to design kernel function $g()$ in the space spanned by the bases. Graph Laplacian L provided eigenvalues and corresponding eigenvector for N number of vertices. This eigenvector is used to define the graph Fourier transform of a function $f(n)$ defined on a vertex n. If signal $f(n)$ lies in the spectrum of the first k eigenvectors, then $f(n)$ is k-band-limited. Graph Fourier transform of a function $f(n)$ is defined on vertices n as:

$$\hat{f}(l) = \sum_{n=1}^{N} f(n)\chi_l^*(n) \tag{1}$$

and

$$f(n) = \sum_{l=1}^{N} \hat{f}(l)\chi_l(n) \tag{2}$$

where χ is a set of eigenvectors that provide orthonormal bases, and χ^* is a conjugate of χ. Graph Fourier coefficient $\hat{f}(l)$ is obtained by forward transform, and the original function $f(n)$ can be reconstructed by the inverse transform.

4.2.3. Problem Setup

We formulated the problem setup as graph signal $f \in \mathbb{R}^{N \times p}$, where measurement p at each node is the one-shot encoding of the node labels, and N is a number of images or nodes. We had an available partial observation at m vertices, where $m << N$. Therefore, partial signal $y \in \mathbb{R}^{m \times p}$, and the goal is to complete the full graph and recover signal f from partially observed y.

4.2.4. Recover Algorithm

As part of the RA [6,9,10], we solved the optimization problem for the estimation g of original signal f:

$$g^* = \arg\min_{g \in \mathbb{R}^n} ||\mathcal{P}_{\Omega}^{-1/2}(Mg - y)||_2^2 + \gamma g^T h(\mathcal{L}) g \tag{3}$$

where $\mathcal{P}_{\Omega} = diag(p(\Omega)), h(\mathcal{L}) = \sum h(\lambda_l)\chi_l\chi_l^T$, $Mf = y$, $p(\Omega)$ is random uniform distribution probability. Sample m nodes from N (random uniform sampling strategy) and the locations where we observed the signal can be denoted as $\omega = \{\omega_1, \omega_2 \ldots \omega_m\}$. On the basis of m observations, a projection matrix [6] $M_{m \times N}$ was built:

$$M_{ij} = \begin{cases} 1, & \text{if } j = \omega_i \\ 0, & \text{o.w.} \end{cases} \tag{4}$$

This framework solves Equation (3) entirely in a dual space by projecting the problem to a low-dimensional space where we search for a solution of size $k << N$ [10]. We took the graph Fourier transform of the function as g, and $\hat{g}_k$ are the first k coefficients. Reformulating Equation (3) using $g = V_k \hat{g}_k$ [10], where $V_k = [\chi_1, \chi_2, ..., \chi_k]$ as:

$$\hat{g}_k^* = \arg \min_{\hat{g}_k \in \mathbb{R}^k} ||\mathcal{P}_\Omega^{-1/2}(M V_k \hat{g}_k - y)||_2^2 + \gamma (V_k \hat{g}_k)^T h(\mathcal{L})(V_k \hat{g}_k) \tag{5}$$

From Equation (4), we recovered low-rank estimation $g^* = V_k \hat{g}_k^*$, that reconstructed our original signal f. Figure 4 shows a toy example of this RA. Here, given a GSP bunny [35] mesh with N = 2503 vertices, we defined a random signal $f \in [0, 1]$ that was band-limited in the spectrum of $\mathcal{L}$ with Gaussian noise of $N(0, 0.1)$, p_1 was the sampling distribution, and sample size m = 600 vertices, which was 20% of the total vertices without replacement. Our estimation g using k = 500 bases is shown in Figure 4. The error between true f and g was extremely small despite using such little data [10].

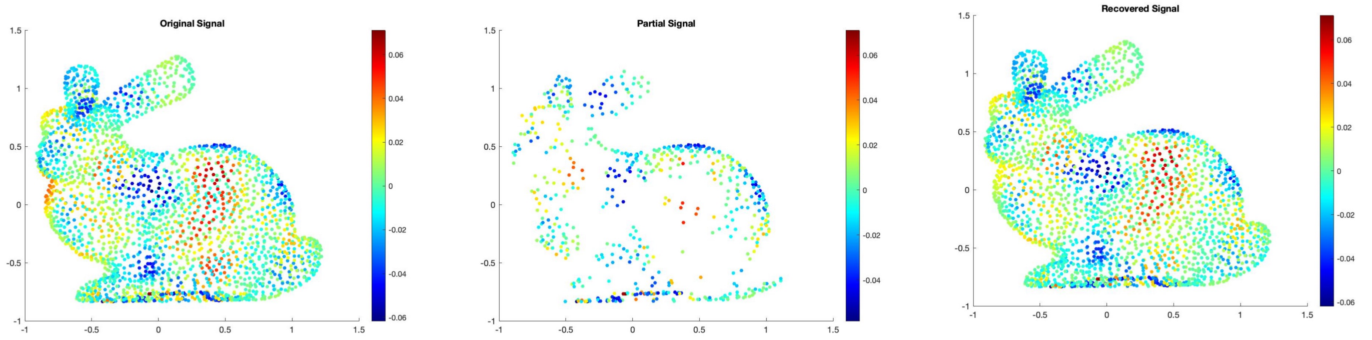

(a) (b) (c)

Figure 4. Toy example of our framework on GSP bunny (N = 2503). (**a**) Band-limited random signal in [0, 1] with noise, (**b**) sampled signal at m = 600 locations out of 2503, (**c**) recovered signal using our method with k = 500.

5. Implementation

CNN-based Siamese networks were first introduced by Koch et al. [18] for one-shot image recognition. Our triple Siamese network architecture was inspired by twin Siamese networks, but with three instead of two parallel networks. These three parallel networks are individually CNN networks. Each CNN network consists of a sequence of convolutional layers, each of which uses a single channel with filters of varying size and a fixed stride of 1. The network applies a ReLU activation function to output feature maps by max-pooling with a filter size and stride of 2. Each layer l takes the following form:

$$h_{1,n} = max(0, W_{l-1,l}^T * h_{1,l-1} + b_l) \tag{6}$$

$$h_{2,n} = max(0, W_{l-1,l}^T * h_{2,l-1} + b_l) \tag{7}$$

$$h_{3,n} = max(0, W_{l-1,l}^T * h_{3,l-1} + b_l) \tag{8}$$

where W is the shared weight matrix, b_l is the shared bias vector, and $*$ is the valid convolutional operation corresponding to each convolutional filter and the input feature maps.

This layer is followed by a fully connected layer, and at the top, we have another layer to compute the L_2 distance between feature vectors generated by three networks; each

L_2 distance is passed through a sigmoid output to obtain the distance between two pairs of inputs.

Figure 5 shows an example of a CNN architecture used in the triple Siamese network, where three of these CNNs are used. Each CNN consists of a sequence of convolutional layers with a single channel and filters of varying size, with a fixed stride of 1. This architecture consists of a number of convolution layers as a multiple of 16. The ReLU activation function is used on the output feature maps, followed by max- pooling with a filter size and stride of 2. The 4096 unit fully connected layer was followed by another layer where we calculated the L_2 distance of each pair.

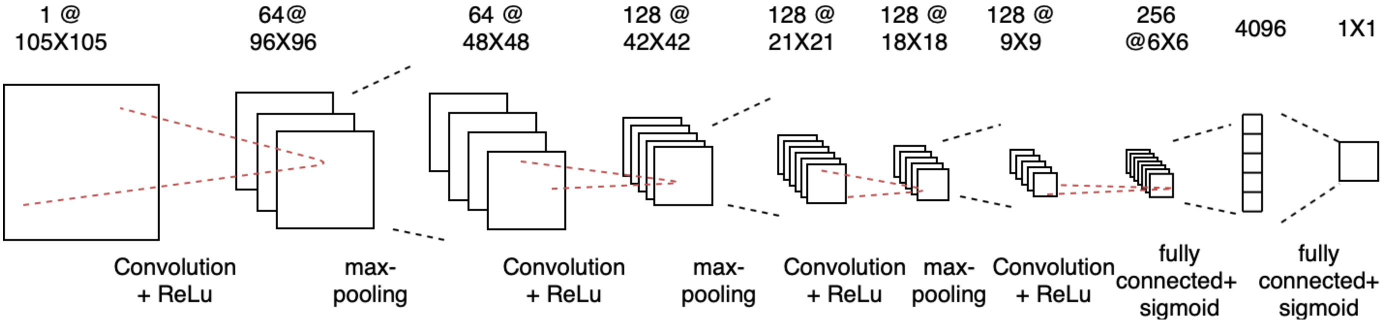

Figure 5. Architecture of a single convolutional neural network used in Siamese network.

5.1. Learning

We initialized all network weights in the convolutional layers from normal distribution with zero mean and a standard deviation of 10^{-2}. Biases were initialized from normal distribution with mean 0.5 and standard deviation 10^{-2}. In the fully connected layers, biases were initialized in the same way as the convolutional layers were, but weights were drawn from a much wider normal distribution with zero mean and standard deviation 2×10^{-2} according to Koch et al. [18]. In the network, training is performed by feeding the network with three samples (x_1, x_2, x_3) at a time when x_2 and x_1 are of the same class, and x_3 is of a different class. The goal is to maximize the distance between x_2 and x_3, and minimize the distance between x_2 and x_1. At the top, there is a comparison layer to compare both similarities, followed by a sigmoid layer to normalize the output in the range of 0 and 1. We used mean square error (MSE) as the loss function. We tested our model with triplet loss function and mean absolute error (MAE). The empirical results showed that our model converged much faster in the case of the Fashion dataset with MSE whereas MAE overfitted our model. Figure 6 shows the training and validation loss for MAE. The back-propagation algorithm ran to simultaneously update the weights for all three networks. Therefore, the loss function is:

$$Loss(s(f_1), s(f_2)) = ||s(f_1), 1 - s(f_2)||_2 \tag{9}$$

where $s(f_1)$ is the sigmoid output of the first distance, and $s(f_2)$ is the sigmoid output of the second distance in Figure 2. Here, f_1 is the L_2-norm of the first two inputs (from the same category), and f_2 is the L_2-norm of the second two inputs (from a different category).

Here, $s(f_1) = 1 - s(f_2)$, as they are formed as a probability. Therefore, Equation (8) can be rewritten as:

$$Loss(s(f_1), s(f_2)) = \alpha.(s(f_1))^2 \tag{10}$$

where α is a constant. Figure 7 shows that the triple Siamese network converged after 150 epochs while training on the Fashion dataset [5]. To obtain optimal results, the triplet could be chosen through three strategies [21]: (i) random mining, (ii) semihard mining, and (iii) hard mining. Our goal was to minimize the distance between positive pairs and maximize the distance between negative pairs. As random mining is the most efficient strategy [21], we used this mining technique for learning.

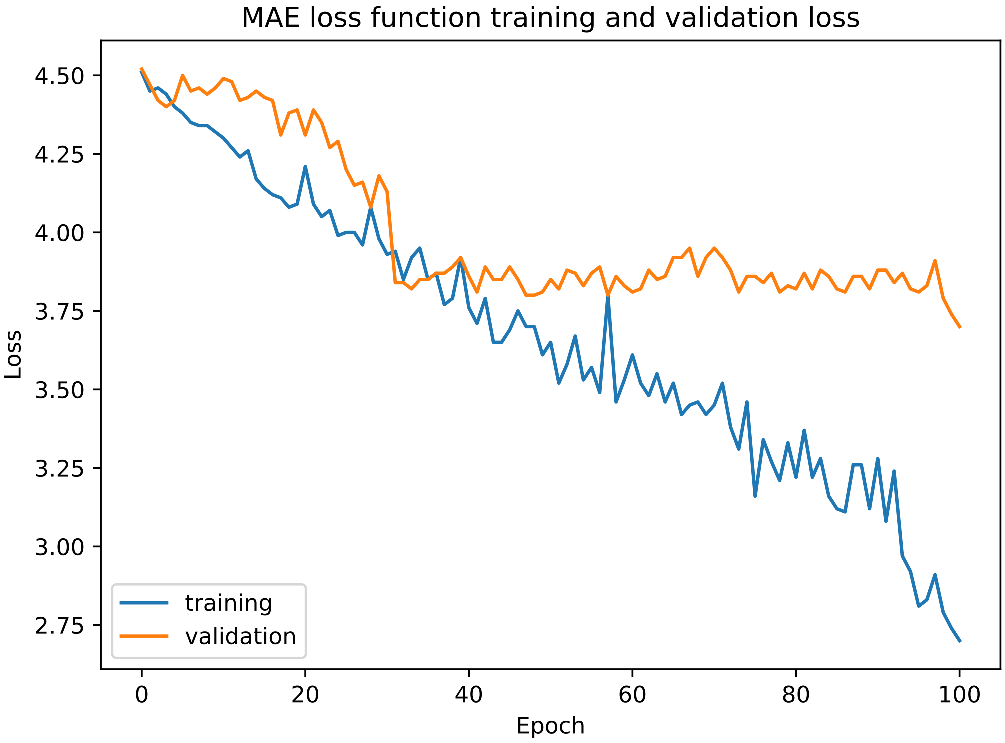

Figure 6. Mean absolute error (MAE) loss function for training and validation.

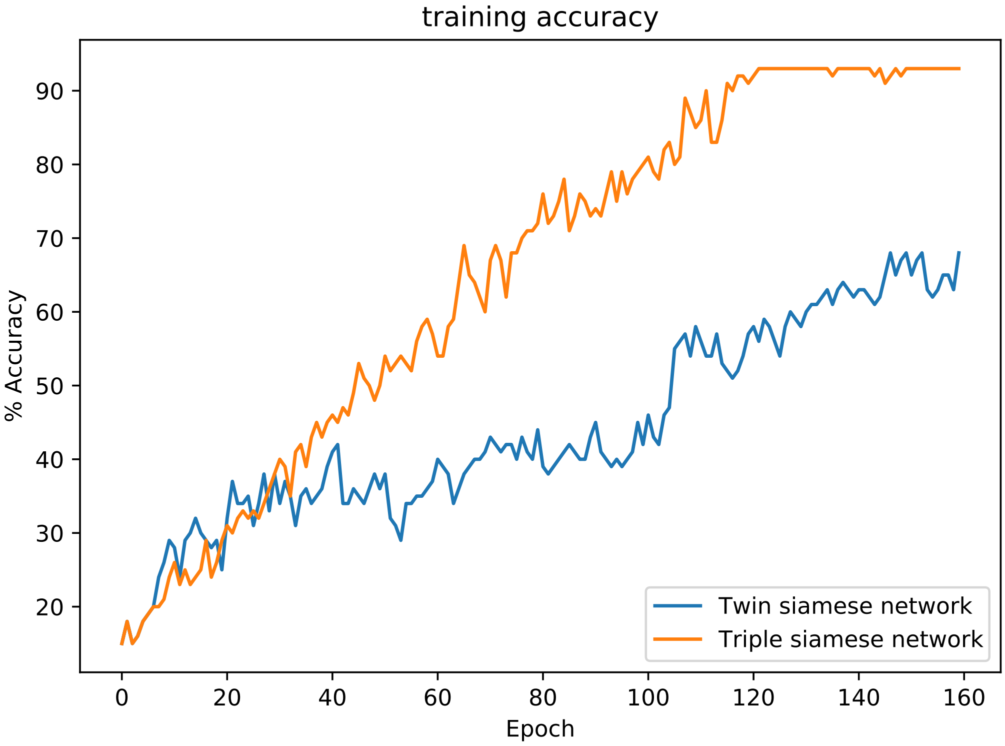

Figure 7. Average training accuracy calculated by performing 2-way one-shot learning.

5.2. Validation

For every pair of input images, this model generated a similarity score between 0 and 1. N-way one-shot methods [18] were applied to measure the performance of this network.

We considered N as 2 to perform one-shot learning, and repeated this k times to calculate percentage of prediction p as:

$$p = \frac{(100 \times n)}{k}\% \tag{11}$$

where n is the number of correct predictions out of k trials. For validation, we used 50 trials. Therefore, k was 50. Figure 8 shows the training and validation loss for MSE.

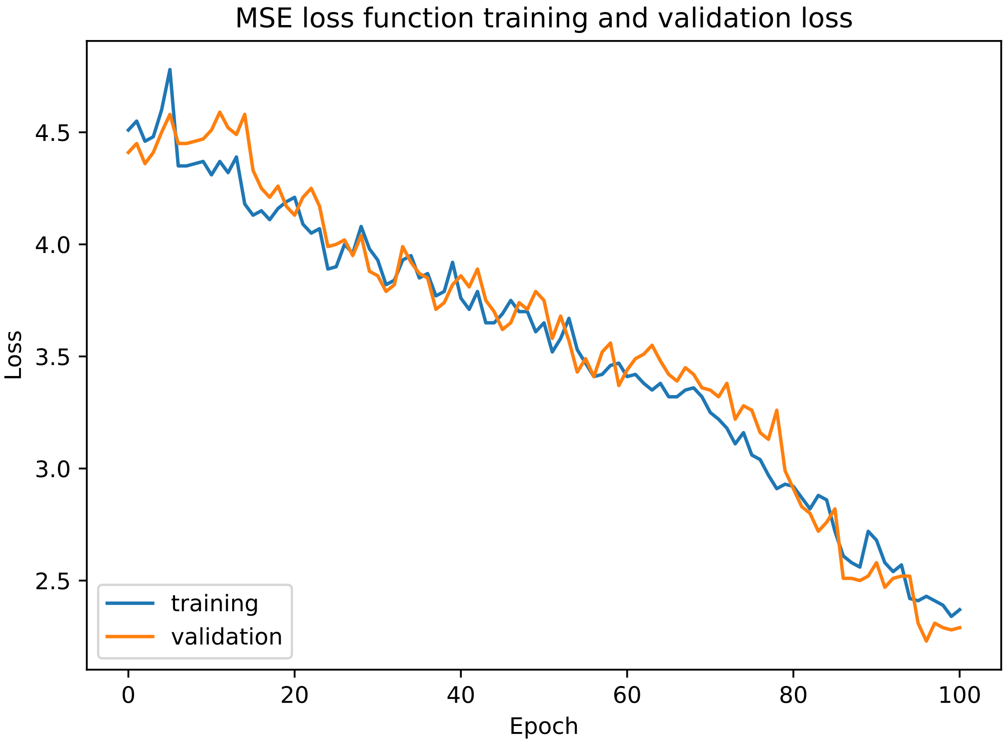

Figure 8. Mean square error (MSE) loss function for training and validation.

5.3. Twin Siamese vs. Triple Siamese Network

The triple Siamese network converges very quickly compared to the twin Siamese network. For example, the triple Siamese network converged in 7.5 min when training on the Fashion dataset, while the twin Siamese network required 1.6 h. Training-system characteristics: CPU 2.3 GHz, 8-Core Intel Core i9, memory 16 GB, 2667 MHz DDR4, GPU AMD Radeon Pro 5500M 4 GB. To detect the distance between each pair of images in our dataset, fewer comparisons were required in the triple Siamese network, and we obtained two distance scores at a time. The triple Siamese network has two parallel layers to calculate the distance metrics, which gives two distance measures at a time. This approach helps to reduce training time in the triple Siamese network. The objective of using three layers of a CNN network is to feed the network with three input images in such a way that two images are from the same class, and the third is from a different class; then, we produce two pairs (two from the same class and the other two from a different class) out of these three input images to calculate two pairs of distance. This model helps to minimize the distance between the two images in the first pair, and maximize the distance between the images in the second pair. Through this model, we captured fine-grained differences between classes that resided very closely in vector space.

6. Experiments and Results

In this section, we demonstrate the results of our algorithm using the Fashion dataset [5]. We downloaded the image dataset from the Myntra Fashion website, out of which we used

1000 images for training, 1000 images for validation, and 4000 images for testing. Figure 9 shows the class distribution of the validation dataset.

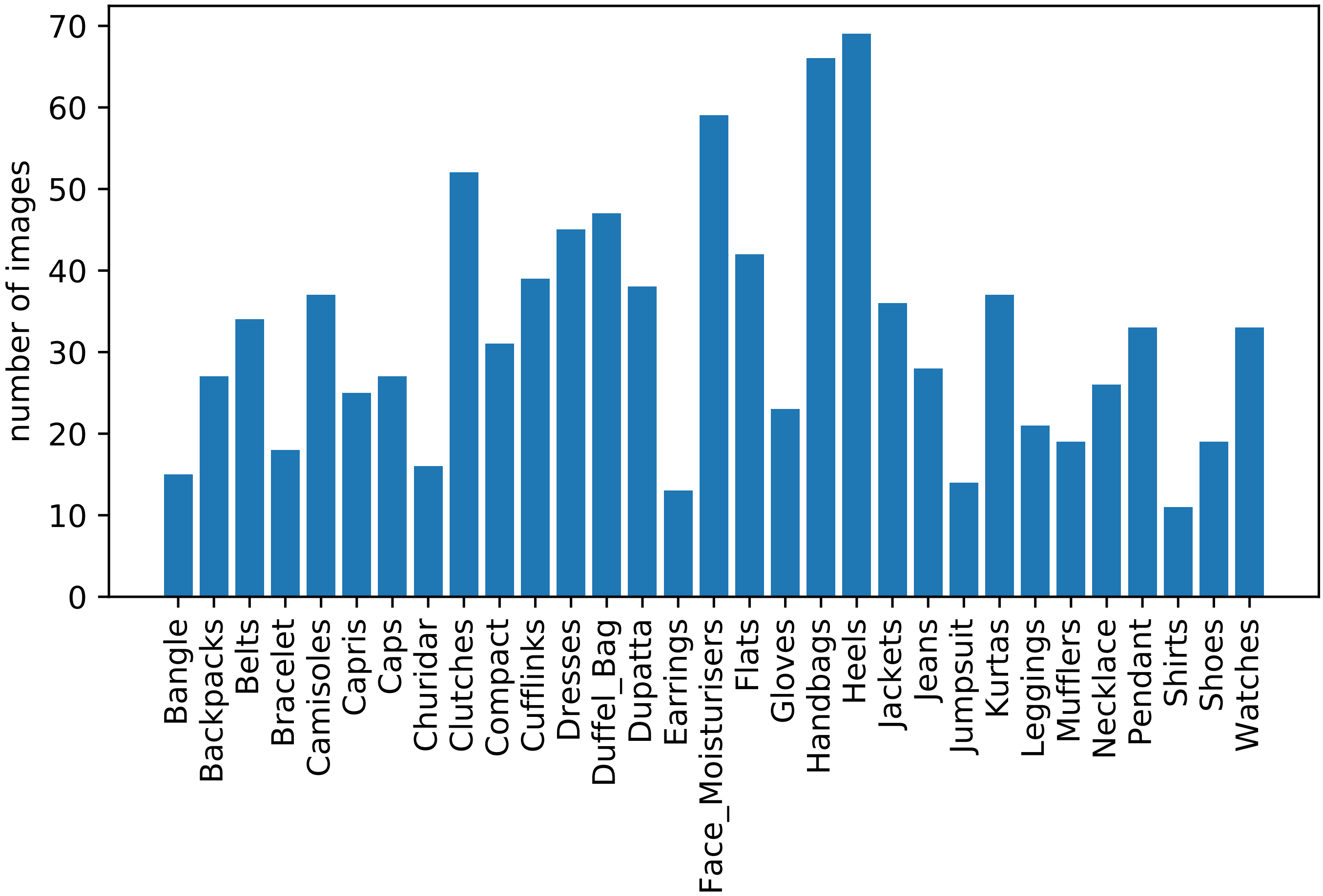

Figure 9. Number of images per category in validation set.

The images had 31 different labels or categories, e.g., handbags, shirts, and shoes. For our experiment, we first created a graph using our triple Siamese network with the images, where images were defined as vertices or nodes, and edges denoted the similarity score between two images. Measurements at each vertex were defined by one-shot encoding of the label vector representing object labels where nonzero elements indicated whether the corresponding objects existed in the image. As our dataset consisted of 31 labels, each measurement was 1×31 vectors. Therefore, we obtained a $f_{4000 \times 31}$ matrix for our entire image dataset, which served as the ground truth of our algorithm. We assumed that our sample m was to be chosen using uniform random sampling and $m << N$. Therefore, m was our partially observed dataset. The k value of our experiment was empirically selected to be 500, which gave optimal accuracy.

We ran our SSL algorithm on this dataset first to create a graph using our proposed triple Siamese network; then, we applied our label-propagation algorithm to recover the signal at each vertex. We compared our algorithm with the baseline twin Siamese network model and k-NN along with a state-of-the-art graph convolutional network. Figure 10 demonstrates the step-by-step operations of our algorithm. Figure 10a indicates the initial state of our dataset with graphical representation. Figure 10b indicates the state after DML, and Figure 10c indicates the final state after label propagation.

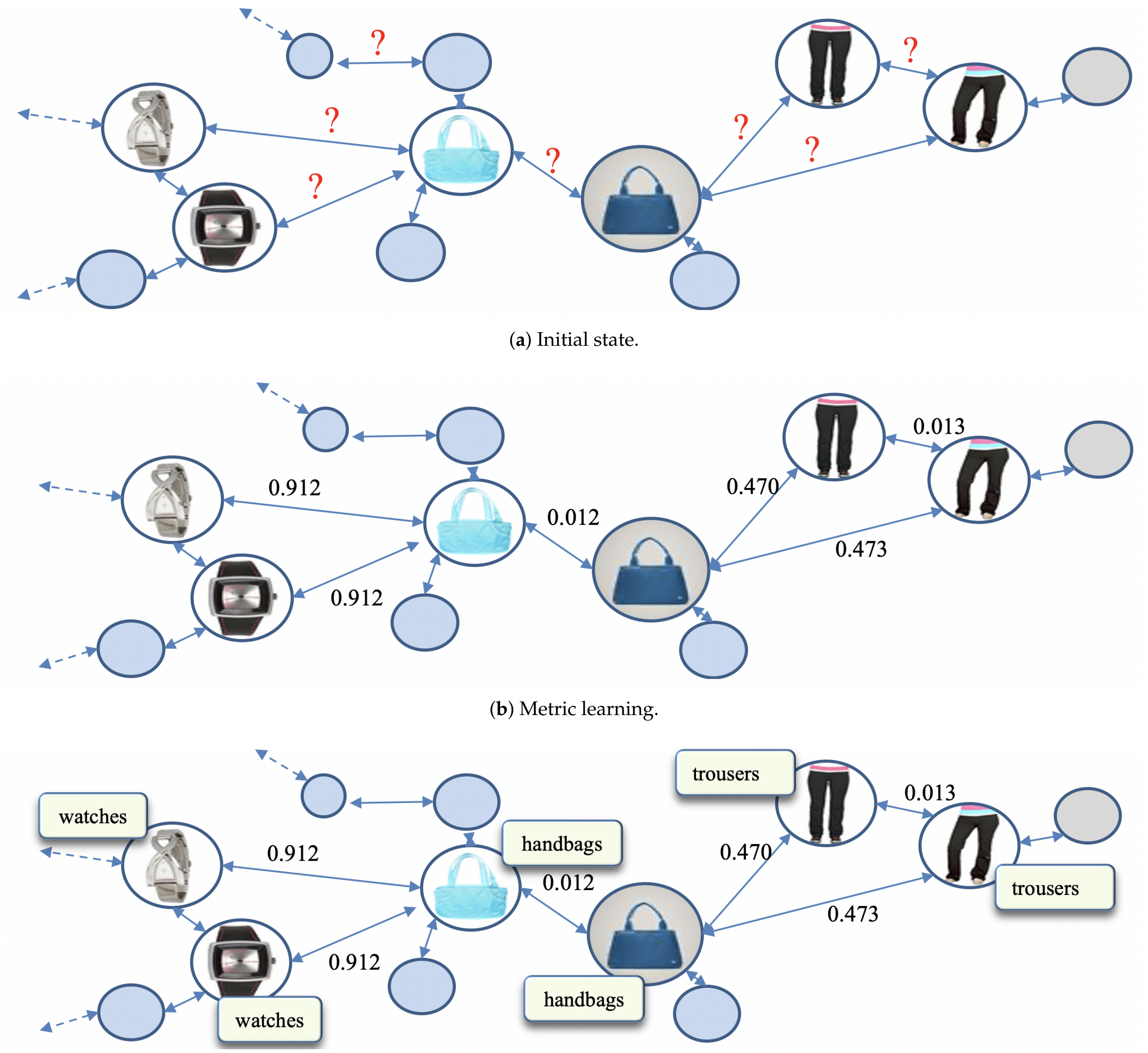

(**a**) Initial state.

(**b**) Metric learning.

(**c**) Label propagation.

Figure 10. Step-by-step operations of proposed method.

Results

After recovering the labels of all images in the Fashion dataset [5], we channeled our output to a sigmoid layer to convert the recovered labels as binary. Since we chose our sample by random uniform sampling, we performed each experiment 50 times to obtain the average accuracy and average precision. We also computed the variance of accuracy and precision of each model for different partial observations. We compared the performance of our algorithm with that of random guess. Random guess [36] is the method of choosing elements at random where they all have an equal chance of being chosen. Our algorithm outperformed other baseline (random guess) and state-of-the-art algorithms, such as twin Siamese, k-nearest neighbors (k-NN), and GNN. We show the performance of our triple Siamese network with RA in Figure 11a,b.

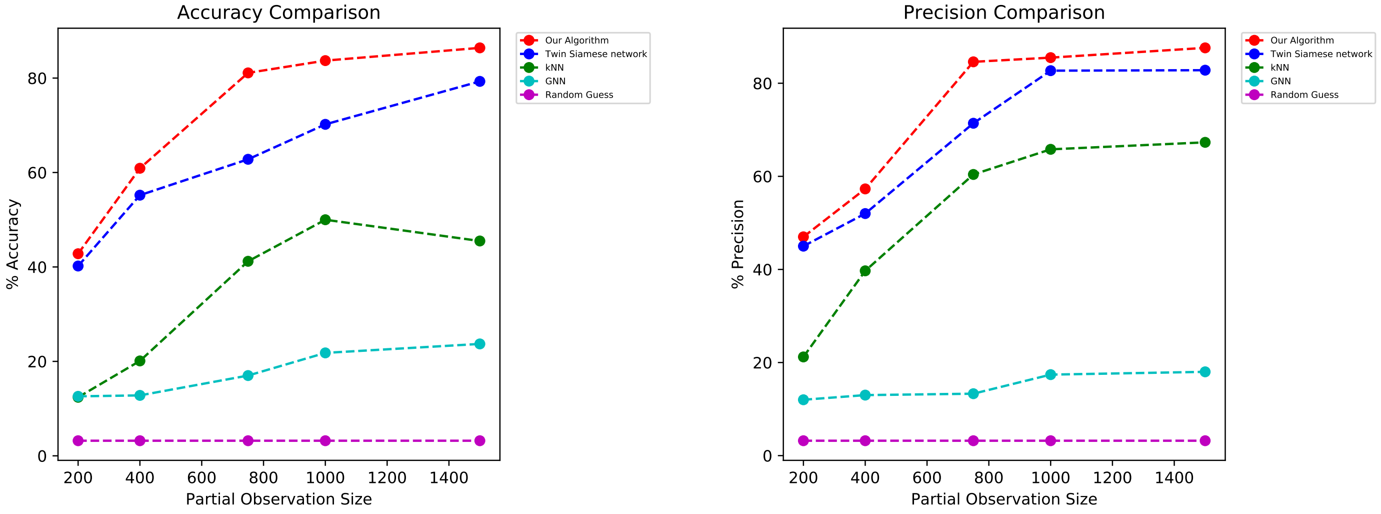

(**a**) Change in accuracy with respect to partial observations.

(**b**) Change in precision with respect to partial observations.

Figure 11. Accuracy and precision comparison with respect to partial observations.

In Figure 11, we observed the performance of our algorithm with different samples or partial-observation sizes. We sampled 5%, 10%, 18.75%, 25%, and 37.5% data points as our partial observations, and recovered the signal using this. With a very small number of samples (10% of sample size), our method performed significantly well compared to other methods.

We compared the performance of our model with different partial-observation sizes, and even with 400 partial-observation sizes out of 4000 data points, our model performed significantly better than other models did. Tables 1 and 2 show the accuracy and precision comparison of our model with respect to other models for different partial-observation sizes, and the variance of the performance metrics with respect to partial observations.

Table 1. Accuracy comparison of our model with other models for different partial-observation (PO) sizes. Note: RA, recover algorithm; k-NN, k-nearest neighbors.

Models	**P.O. 400**		**P.O. 750**		**P.O. 1000**		**P.O. 1500**	
	Acc	**Var**	**Acc**	**Var**	**Acc**	**Var**	**Acc**	**Var**
Triple Siamese net and RA (our method)	**60.91%**	29.37	**81.1%**	22.45	**83.7%**	31.83	**86.4%**	27.32
Twin Siamese net and RA [18]	55.23	21.45	62.8%	12.87	70.2%	22.75	79.3%	17.20
Triple Siamese net and k-NN [37]	20.1	13.8	41.6%	26.92	50%	23.66	45.5%	9.25
Graph convolutional network [24]	12.81	15.2	17%	10.01	21.8%	17.21	23.7%	22.90

Table 2. Precision Comparison of our model with other models for different partial-observation sizes.

Models	**P.O. 400**		**P.O. 750**		**P.O. 1000**		**P.O. 1500**	
	Acc	**Var**	**Acc**	**Var**	**Acc**	**Var**	**Acc**	**Var**
Triple Siamese net and RA(Our method)	**57.32%**	15.4	**84.6%**	18.67	**85.5%**	10.49	**87.6%**	9.41
Twin Siamese net and RA [18]	52%	17.77	71.4%	16.33	82.7%	17.71	82.8%	12.58
Triple Siamese net and k-NN [37]	39.71%	17.32	60.4%	32.79	65.8%	23.36	67.3%	18.63
Graph convolutional network [24]	13.32%	16.51	13.3%	15.62	17.4%	17.49	18%	17.22

7. Conclusions

In this work, we introduce a novel approach for SSL in the Fashion dataset, where we had a limited amount of labeled data to train our model. As the backbone of our algorithm, we assumed that similar data points resided close to each other in vector space, and different data points reside far away from each other in vector space. We then discussed a novel algorithm for DML approaches to retrieve similarity measures from image-feature vectors. Our DML model quickly converged and was able to capture fine-grain differences between class labels. We also discussed the concept of spectral graph theory and the application of harmonic analysis on the graph signal to recover the signal from our partially observed graph data. Our algorithm performed significantly better than GCN and the twin Siamese network did, even for the very small amount of labeled data in the Fashion dataset.

We plan to extend our work towards designing a generalized triple Siamese network in combination with transfer learning [38], and evaluating its performance on other standard image datasets in the same or different domains, such as the Fashion-MNIST dataset [39] and ImageNet [40].

In the future, this work can be extended using different DML architectures such as FaceNet [20]. This architecture is mainly used for classifying facial image datasets. The loss function used in this model was triplet loss function, which can be further extended in our framework.

Furthermore, this work can be extended towards other modalities using multimodal fusion architectures [41], and can be compared with our framework for measuring performance. Moreover, we aim to extend this work using active learning [42] and to evaluate the performance of the framework.

Author Contributions: Conceptualization, D.B. and W.H.K.; methodology, formal analysis, design, validation, D.B.; writing—original-draft preparation, D.B.; writing—review and editing, D.B., M.K. and W.H.K.; supervision, project administration, and funding acquisition, W.H.K. All authors have read and agreed to the published version of the manuscript.

Funding: This research was supported by NSF IIS CRII 1948510, NIH R01 AG059312, and IITP-2020-2015-0-00742.

Institutional Review Board Statement: Not applicable.

Informed Consent Statement: Not applicable.

Conflicts of Interest: The authors declare no conflict of interest.

Abbreviations

The following abbreviations are used in this manuscript:

AI	Artificial intelligence
ML	Machine learning
DML	Distance metric learning
CNN	Convolutional neural network
MSE	Mean square error
SSL	Semisupervised learning
ReLU	Rectified linear unit
GNN	Graph neural network
k-NN	k-nearest neighbors
MAE	Mean absolute error
RA	Recover algorithm

References

1. Niculescu-Mizil, A.; Caruana, R. Predicting good probabilities with supervised learning. In Proceedings of the ICML '05, Bonn, Germany, 7–11 August 2005.
2. Kotsiantis, S.B. Supervised Machine Learning: A Review of Classification Techniques. In Proceedings of the 2007 Conference on Emerging Artificial Intelligence Applications in Computer Engineering: Real Word AI Systems with Applications in EHealth, HCI, Information Retrieval and Pervasive Technologies, Amsterdam, The Netherlands, 14–16 June 2007; pp. 3–24.
3. Loog, M. Supervised Classification: Quite a Brief Overview. *arXiv* **2017**, arXiv:cs.LG/1710.09230.
4. Stephen, P.; Jaganathan, S. Linear regression for pattern recognition. In Proceedings of the 2014 International Conference on Green Computing Communication and Electrical Engineering (ICGCCEE), Coimbatore, India, 6–8 March 2014; pp. 1–6. [CrossRef]
5. Param, A. Fashion Product Images (Small). 2019. Available online: https://www.kaggle.com/paramaggarwal/fashion-product-images-small (accessed on 20 January 2021).
6. Kim, W.H.; Jalal, M.; Hwang, S.; Johnson, S.C.; Singh, V. Online Graph Completion: Multivariate Signal Recovery in Computer Vision. In Proceedings of the IEEE Conference on Computer Vision and Pattern Recognition (CVPR), Honolulu, HI, USA, 21–26 July 2017.
7. van Engelen, J.E.; Hoos, H. A survey on semi-supervised learning. *Mach. Learn.* **2019**, *109*, 373–440. [CrossRef]
8. Iscen, A.; Tolias, G.; Avrithis, Y.; Chum, O. Label Propagation for Deep Semi-supervised Learning. In Proceedings of the IEEE/CVF Conference on Computer Vision and Pattern Recognition (CVPR), Long Beach, CA, USA, 16–20 June 2019; pp. 5070–5079.
9. Puy, G.; Tremblay, N.; Gribonval, R.; Vandergheynst, P. Random sampling of bandlimited signals on graphs. In Proceedings of the NIPS2015 Workshop on Multiresolution Methods for Large Scale Learning, Montréal, QC, Canada, 12 December 2015.
10. Kim, W.H.; Hwang, S.J.; Adluru, N.; Johnson, S.C.; Singh, V. Adaptive Signal Recovery on Graphs via Harmonic Analysis for Experimental Design in Neuroimaging. In Proceedings of the Computer Vision—ECCV 2016—14th European Conference, Amsterdam, The Netherlands, 11–14 October 2016; Part VI; Lecture Notes in Computer Science; Leibe, B., Matas, J., Sebe, N., Welling, M., Eds.; Springer: Berlin/Heidelberg, Germany, 2016; Volume 9910, pp. 188–205. [CrossRef]
11. Bronstein, M.M.; Bruna, J.; LeCun, Y.; Szlam, A.; Vandergheynst, P. Geometric Deep Learning: Going beyond Euclidean data. *IEEE Signal Process. Mag.* **2017**, *34*, 18–42. [CrossRef]
12. Malkov, Y.A.; Yashunin, D.A. Efficient and robust approximate nearest neighbor search using Hierarchical Navigable Small World graphs. *IEEE Trans. Pattern Anal. Mach. Intell.* **2020**, *42*, 824–836. [CrossRef] [PubMed]
13. Saito, K.; Kim, D.; Sclaroff, S.; Darrell, T.; Saenko, K. Semi-supervised Domain Adaptation via Minimax Entropy. In Proceedings of the IEEE/CVF International Conference on Computer Vision (ICCV), Seoul, Korea, 27 October–2 November 2019; pp. 8050–8058.
14. Zhai, X.; Oliver, A.; Kolesnikov, A.; Beyer, L. S4L: Self-Supervised Semi-Supervised Learning. In Proceedings of the IEEE/CVF International Conference on Computer Vision (ICCV), Seoul, Korea, 27 October–2 November 2019; pp. 1476–1485.
15. Bromley, J.; Guyon, I.; LeCun, Y.; Säckinger, E.; Shah, R. Signature Verification using a "Siamese" Time Delay Neural Network. In *Advances in Neural Information Processing Systems*; Cowan, J., Tesauro, G., Alspector, J., Eds.; Morgan-Kaufmann: Burlington, MA, USA, 1994; Volume 6, pp. 737–744.
16. Fei-Fei, L.; Fergus, R.; Perona, P. One-shot learning of object categories. *IEEE Trans. Pattern Anal. Mach. Intell.* **2006**, *28*, 594–611. [CrossRef]
17. Lake, B.M.; Salakhutdinov, R.; Tenenbaum, J.B. Human-level concept learning through probabilistic program induction. *Science* **2015**, *350*, 1332–1338. [CrossRef]
18. Koch, G.; Zemel, R.; Salakhutdinov, R. Siamese Neural Networks for One-shot Image Recognition. In Proceedings of the ICML Deep Learning Workshop, Lille Grand Palais, France, 6–11 July 2015.
19. Vinyals, O.; Blundell, C.; Lillicrap, T.; Kavukcuoglu, K.; Wierstra, D. Matching Networks for One Shot Learning. *Adv. Neural Inf. Process. Syst.* **2016**, *29*, 3630–3638.
20. Schroff, F.; Kalenichenko, D.; Philbin, J. FaceNet: A unified embedding for face recognition and clustering. In Proceedings of the 2015 IEEE Conference on Computer Vision and Pattern Recognition (CVPR), Boston, MA, USA, 8–10 June 2015. [CrossRef]
21. Kertész, G. Metric Embedding Learning on Multi-Directional Projections. *Algorithms* **2020**, *13*, 133. [CrossRef]
22. Gori, M.; Monfardini, G.; Scarselli, F. A new model for learning in graph domains. In Proceedings of the 2005 IEEE International Joint Conference on Neural Networks, Montreal, QC, Canada, 31 July–4 August 2005; Volume 2, pp. 729–734.
23. Doersch, C. Tutorial on Variational Autoencoders. *arXiv* **2016**, arXiv:stat.ML/1606.05908.
24. Kipf, T.N.; Welling, M. Variational Graph Auto-Encoders. *arXiv* **2016**, arXiv:stat.ML/1611.07308.
25. Goodfellow, I.J.; Pouget-Abadie, J.; Mirza, M.; Xu, B.; Warde-Farley, D.; Ozair, S.; Courville, A.; Bengio, Y. Generative Adversarial Networks. *arXiv* **2014**, arXiv:stat.ML/1406.2661.
26. Odena, A. Semi-Supervised Learning with Generative Adversarial Networks. *arXiv* **2016**, arXiv:stat.ML/1606.01583.
27. Salimans, T.; Goodfellow, I.; Zaremba, W.; Cheung, V.; Radford, A.; Chen, X. Improved Techniques for Training GANs. *arXiv* **2016**, arXiv:cs.LG/1606.03498.
28. Kipf, T.N.; Welling, M. Semi-Supervised Classification with Graph Convolutional Networks. *arXiv* **2016**, arXiv:1609.02907.
29. Chang, M.B.; Ullman, T.; Torralba, A.; Tenenbaum, J.B. A Compositional Object-Based Approach to Learning Physical Dynamics. *arXiv* **2016**, arXiv:1612.00341.
30. Duvenaud, D.; Maclaurin, D.; Aguilera-Iparraguirre, J.; Gómez-Bombarelli, R.; Hirzel, T.; Aspuru-Guzik, A.; Adams, R.P. Convolutional Networks on Graphs for Learning Molecular Fingerprints. *Adv. Neural Inf. Process. Syst.* **2015**, *28*, 2224–2232.

31. Kearnes, S.M.; McCloskey, K.; Berndl, M.; Pande, V.S.; Riley, P. Molecular graph convolutions: Moving beyond fingerprints. *J. Comput. Aided Mol. Des.* **2016**, *30*, 595–608. [CrossRef]
32. Gilmer, J.; Schoenholz, S.S.; Riley, P.F.; Vinyals, O.; Dahl, G.E. Neural message passing for quantum chemistry. In Proceedings of the 34th International Conference on Machine Learning, Sydney, Australia, 6–11 August 2017; Volume 70, pp. 1263–1272.
33. Appalaraju, S.; Chaoji, V. Image similarity using Deep CNN and Curriculum Learning. *arXiv* **2017**, arXiv:1709.08761.
34. Hammond, D.K.; Vandergheynst, P.; Gribonval, R. Wavelets on Graphs via Spectral Graph Theory. *App. Comput. Harmonic Anal.* **2011**, *30*, 129–150. [CrossRef]
35. Turk, G.; Levoy, M. Zippered Polygon Meshes from Range Images. In Proceedings of the 21st Annual Conference on Computer Graphics and Interactive Techniques (SIGGRAPH '94), Orlando, FL, USA, 24–29 July 1994; pp. 311–318. [CrossRef]
36. Frary, R.B.; Cross, L.H.; Lowry, S.R. Random guessing, correction for guessing, and reliability of multiple-choice test scores. *J. Exp. Educ.* **1977**, *46*, 11–15. [CrossRef]
37. Hui, G.G.; Wang, H.; Bell, D.; Bi, Y.; Greer, K. KNN Model-Based Approach in Classification. In Proceedings of the OTM Confederated International Conferences On the Move to Meaningful Internet Systems, Catania, Italy, 3–7 November 2003.
38. Tan, C.; Sun, F.; Kong, T.; Zhang, W.; Yang, C.; Liu, C. A Survey on Deep Transfer Learning. In Proceedings of the International Conference on Artificial Neural Networks, Rhodes, Greece, 4–7 October 2018.
39. Xiao, H.; Rasul, K.; Vollgraf, R. Fashion-MNIST: A Novel Image Dataset for Benchmarking Machine Learning Algorithms. *arXiv* **2017**, arXiv:1708.07747.
40. Deng, J.; Dong, W.; Socher, R.; Li, L.J.; Li, K.; Fei-Fei, L. ImageNet: A Large-Scale Hierarchical Image Database. In Proceedings of the 2009 IEEE Conference on Computer Vision and Pattern Recognition (CVPR09), Miami, FL, USA, 20–25 June 2009.
41. Vielzeuf, V.; Lechervy, A.; Pateux, S.; Jurie, F. CentralNet: A Multilayer Approach for Multimodal Fusion. In Proceedings of the European Conference on Computer Vision (ECCV), Munich, Germany, 8–14 September 2018.
42. Settles, B. *Active Learning Literature Survey (Computer Sciences Technical Report 1648)*; University of Wisconsin-Madison: Madison, WI, USA, 2009.